The American Journal of Pathology, Vol. 193, No. 7, July 2023

ELSEVIER

The American Journal of PATHOLOGY

ajp.amjpathol.org

METABOLIC, ENDOCRINE, AND GENITOURINARY PATHOBIOLOGY

Systemic Reduction of Glut1 Normalizes Retinal Dysfunction, Inflammation, and Oxidative Stress in the Retina of Spontaneous Type 2 Diabetic Mice

Jacob J. Aiello,* Maislin C. Bogart,* Wai-Ting Chan,* Nicholas C. Holoman,* Timothy D. Trobenter,* Chloe E. Relf,* Dana M. Kleinman,* Darryl C. De Vivo,† and Ivy S. Samuels*‡

From the Louis Stokes Cleveland VA Medical Center, VA Northeast Ohio Healthcare System, Cleveland, Ohio; the Departments of Neurology and Pediatrics,† Columbia University Irving Medical Center, New York, New York; and the Department of Ophthalmic Research,‡ Cole Eye Institute, Cleveland, Ohio*

Accepted for publication April 4, 2023.

Address correspondence to Ivy S. Samuels, Ph.D., Louis Stokes Cleveland VA Medical Center, 151W Research Service, VA Northeast Ohio Healthcare System, 10901 E. Blvd., Cleveland, OH 44106. E-mail: ivy.samuels@va.gov or samueli@ccf.org.

Defects in the light-evoked responses of the retina occur early in the sequalae of diabetic retinopathy (DR). These defects, identified through the electroretinogram (ERG), represent dysfunction of retinal neurons and the retinal pigment epithelium and are commonly identifiable at the timing of, or almost immediately following, diabetes diagnosis. Recently, systemic reduction of the facilitated glucose transporter type 1, Glut1, in type 1 diabetic mice was shown to reduce retinal sorbitol accumulation, mitigate ERG defects, and prevent retinal oxidative stress and inflammation. Herein, the study investigated whether systemic reduction of Glut1 also diminished hallmarks of DR in type 2 diabetic mice. Transgenic nondiabetic *Lepr*$^{db/+}$ and spontaneously diabetic *Lepr*$^{db/db}$ mice that expressed wild-type (*Glut1*$^{+/+}$) or systemically reduced levels of Glut1 (*Glut1*$^{+/-}$) were aged and subjected to standard strobe flash electroretinography and c-wave analysis before evaluation of inflammatory cytokines and oxidative stress molecules. Although *Lepr*$^{db/db}$*Glut1*$^{+/-}$ mice still displayed overt obesity and diabetes, no scotopic, photopic, or c-wave ERG defects were present through 16 weeks of age, and expression of inflammatory cytokines and oxidative stress molecules was also normalized. These findings suggest that systemic reduction of Glut1 is sufficient to prevent functional retinal pathophysiology in type 2 diabetes. Targeted, moderate reductions of Glut1 or inhibition of Glut1 activity in the retina of diabetic patients should be considered as a novel therapeutic strategy to prevent development and progression of DR. *(Am J Pathol 2023, 193: 927–938; https://doi.org/10.1016/j.ajpath.2023.04.003)*

Diabetes affects >537 million adults worldwide, accounting for 11.5% of the global health expenditure (International Diabetes Federation Diabetes Atlas, 10th edition, 2021). Despite differing etiology of type 1 (inability to produce insulin) and type 2 (insulin-resistant) diabetes, the characteristics of diabetic retinopathy (DR) are not distinguished between the two diseases. Nevertheless, because approximately 90% to 95% of all diabetes cases are classified as type 2 diabetes (T2D), therapeutic interventions for DR need to be tested in and specifically addressed in this group (CDC National Diabetes Statistics Report, *https://www.cdc.gov/diabetes/data/statistics-report/index.html*, last accessed March 1, 2023).

Inhibition of glucose transport has long been a target for the microvascular complications of diabetes. Recently, the inhibition of *Sglt2*, the sodium-glucose cotransporter, has been investigated for the prevention of DR, diabetic kidney disease, and diabetic neuropathy. However, the findings

Supported by the US Department of Veterans Affairs Biomedical Laboratory Research and Development Service VA Merit Award number BX005844-01 (I.S.S.), NIH P30 EY025585, Research to Prevent Blindness Challenge grant, Cleveland Eye Bank Foundation grant, and Cleveland Clinic Foundation funds.

Disclosures: None declared. All co-authors have seen and agree with the contents of the manuscript, and there is no financial interest to report.

Portions of this work were presented as an abstract at the 2019 Association for Research in Vision and Ophthalmology Annual Meeting, April 28 to May 2, 2019, Vancouver, BC, Canada.

https://doi.org/10.1016/j.ajpath.2023.04.003

from these studies are mixed.[1–5] Moreover, a recent study found reduced *Sglt2* levels in peripheral blood mononuclear cells of patients with proliferative diabetic retinopathy, suggesting that although targeting of glucose is desired, inhibition of *Sglt2* may not be an effective therapeutic for prevention of DR.[6] Recent work demonstrated that systemic or retina-specific reduction of the primary facilitative glucose transporter in the retina and retinal pigment epithelium (RPE), Glut1 (*Slc2a1*), attenuated hallmarks of DR in the streptozotocin mouse model of type 1 diabetes at both acute (2 and 4 weeks) and prolonged (12 weeks) time points. This included a normalization of reductions in electroretinogram (ERG) component amplitudes, reduced accumulation of the neurotoxic polyol, sorbitol, in the retina, and a marked reduction in inflammation/oxidative stress molecules. The reversal of these outcome measures was found at both early (4 weeks) and sustained (12 weeks) durations of diabetes.[7] To determine whether systemic reduction of Glut1 levels in a mouse model of T2D also prevents pathologic characteristics of DR, Glut1 expression was genetically reduced in the $Lepr^{db/db}$ mouse by crossing it with a $Glut1^{+/-}$ line. Nondiabetic $Glut1^{+/-}Lepr^{db/+}$ mice displayed 40% reduced Glut1 levels throughout the retina, compared with $Glut1^{+/+}Lepr^{db/+}$ littermates. $Glut1^{+/+}Lepr^{db/db}$ mice exhibited overt obesity and hyperglycemia compared with nondiabetic $Glut1^{+/+}Lepr^{db/+}$ mice. Although $Glut1^{+/-}Lepr^{db/db}$ mice remained diabetic and obese, they also exhibited a significant reduction of Glut1 in the retina. All four genotypes underwent strobe flash electroretinography and c-wave analysis at 8 and 16 weeks of age. At both time points, the reduction in Glut1 levels ($Glut1^{+/-}$) in diabetic ($Lepr^{db/db}$) mice normalized ERG component amplitudes, including the photoreceptor-derived a-wave, the bipolar cell-dependent b-wave, and the RPE-dependent c-wave. Retinal oscillatory potentials were also normalized at 8 and 16 weeks of age. Expression of inflammatory cytokines and markers of oxidative stress molecules was similarly attenuated in diabetic mice by the systemic reduction of Glut1.

Materials and Methods

Mice

$Lepr^{db/db}$ mice of the C57BLKS background were purchased from The Jackson Laboratory (Bar Harbor, ME; number 000642). $Glut1^{+/-}$ mice were kindly provided by Darryl De Vivo (Columbia University, New York, NY). Mice were intercrossed to generate control ($Lepr^{db/+}$) and diabetic ($Lepr^{db/db}$) mice with one ($Glut1^{+/-}$) or two ($Glut1^{+/+}$) wild-type Glut1 alleles. Both male and female mice were used. All animals were maintained on a 12-hour light/dark cycle and provided food *ad libitum*. All experiments were performed in accordance with the Institutional Animal Care and Use Committee at the Louis Stokes Cleveland VA Medical Center (Cleveland, OH) and followed the Association for Research in Vision and Ophthalmology Guidelines for Use of Animals in Ophthalmic and Vision Research.

Genotyping

The $Glut1^{+/+}$ and $Glut1^{+/-}$ alleles were identified using the following primers: wild-type forward, 5′-CCATAAAGTCA GAAATGGAGGGAGGTGGTGGT-3′; wild-type reverse, 5′-GCGAGACGGAGAACGGACGCGCTGTAACTA-3′; and mutant reverse, 5′-CTACCGGTGGATGTGGAAT GTGTGCGAGGC-3′.

The $Lepr^{db/db}$ allele was identified by high-resolution melt analysis using the following primers: forward, 5′-TGACCACTACAGATGAACCCA-3′; and reverse, 5′-GTCATTCAAACCATAGTTTAGGTTTGT-3′.

Electroretinography

After overnight dark adaptation, mice were anesthetized with 65 mg/kg sodium pentobarbital. Eye drops were used to anesthetize the cornea (1% proparacaine HCl) and to dilate the pupil (2.5% phenylephrine HCl, 1% tropicamide, and 1% cyclopentolate HCl). Mice were placed on a temperature-regulated heating pad throughout the recording session, which was performed as previously described.[7] In brief, ERGs were recorded in response to strobe flash stimuli presented in the dark by an Espion E3 ColorDome Full Field Ganzfeld (Diagnosys, Lowell, MA). An Ag/AgCl electrode in contact with the cornea was referenced to an Ag/AgCl pellet electrode placed in the mouth of the mouse, and a ground lead was placed in the tail. Scotopic responses were obtained in the dark with 10 steps of a white-light flash stimulus, ranging from -3.6 log cd.s/m^2 to 2.1 log cd.s/m^2. The duration of the interstimulus intervals increased from 4 seconds for low-luminance flashes to 90 seconds for the highest stimuli. Two minutes following the scotopic ERG, a 10-second white light stimulus (5 cd/m^2) was presented to elicit the c-wave. After 7 minutes of light adaptation, cone ERGs were recorded with strobe-flash stimuli (-1 to 2 log cd $\cdot$ s/m^2) superimposed on the adapting field. Amplitude of the a-wave was measured at 8.3 milliseconds following the stimulus. Amplitude of the b-wave was calculated by summing the amplitude of the a-wave at 8.3 milliseconds with the peak of the waveform after the oscillatory potentials ($\geq$40 milliseconds). Light-adapted response amplitudes were calculated by summing the peak of the waveform with the amplitude at 8.3 milliseconds. Oscillatory potentials (OPs) were filtered from the strobe flash responses by the Diagnosys program. OP amplitude was determined by measuring the change in amplitude from the preceding trough to the peak of each potential. Amplitude of the c-wave was determined by subtracting the average baseline amplitude from the maximal response following the b-wave.

Table 1 Antibodies

Antigen	Supplier	Catalog no.	Species	Dilution: WB analysis	Dilution: IHC
Actin	Cell Signaling	3700S	Mouse	1:1000	
Glut1	Millipore Sigma (St. Louis, MO)	07-1401	Rabbit	1:2000	1:500
Glutamine synthetase	BD Biosciences (San Jose, CA)	610517	Mouse		1:500
Alexa Fluor 488	Invitrogen (Waltham, MA)	A11008	Rabbit		1:500
Alexa Fluor 594	Invitrogen	A11032	Mouse		1:500
Donkey anti-mouse 800CW	Li-Cor	926-32212	Mouse	1:10,000	
Donkey anti-rabbit 680RD	Li-Cor	926-68073	Rabbit	1:10,000	

IHC, immunohistochemistry; WB, Western blot.

Western Blot Analysis

Retinas were isolated from enucleated eyecups, and protein was extracted using 100 μL per retina in radioimmunoprecipitation assay buffer (Cell Signaling, Danvers, MA; number 9806S) with Roche cOmplete ULTRA Protease Inhibitor (Sigma, St. Louis, MO; number 5892970001). Retinal samples were homogenized by trituration with a P200 pipette. Samples were placed on ice for 30 minutes with intermittent vortexing every 10 minutes. The samples were centrifuged at 18,626 × *g* for 20 minutes, and the supernatants were removed for protein quantification by BCA Protein Assay (Thermo Scientific, Rockford, IL; number 23208).

A total of 15 μg of retina protein was loaded on 4% to 15% Mini-PROTEAN TGX gels (BioRad, Hercules, CA; number 4561083) with diluted 6× Laemelli SDS reducing sample buffer. Gels were run for approximately 90 minutes at 125 V and transferred electrophoretically onto polyvinylidene difluoride transfer membranes (activated with methanol) at 100 V for 1 hour. Membranes were then incubated for 1 hour at room temperature in Odyssey blocking buffer (Li-Cor, Lincoln, NE; number 927-500) and incubated overnight with primary antibodies at 4°C in Odyssey blocking buffer. See Table 1 for sources and dilutions of all primary and secondary antibodies used for Western blot analysis. Membranes were washed 3 × 5 minutes with tris-buffered saline with 0.1% Tween 20 and incubated for 1 hour in the dark with Li-Cor IRdye secondary antibodies (1:10,000) in Odyssey blocking buffer + 0.2% Tween 20 + 0.01% SDS. Blots were washed 3 × 5 minutes in tris-buffered saline with Tween 20 at room temperature in the dark, rinsed with tris-buffered saline, and imaged with an Odyssey CLx Infrared Imaging System (Li-Cor). Densitometry was performed with Li-Cor Image Studio Software.

Immunohistochemistry

Enucleated eyes were fixed in 4% paraformaldehyde, and eyecups were prepared by removal of the cornea and lens. Tissue was fixed for 1 to 4 hours at room temperature before equilibration in sucrose solutions (10% for 1 hour; 20% for 1 hour; and 30% overnight). Equilibrated eyecups were embedded in Tissue Tek OCT Compound (Sakura Finetek USA, Torrence, CA), frozen on dry ice, and cryosectioned at 10 μm. Slides were stored at −20°C and brought to room temperature before rehydration with 1 × phosphate-buffered saline (PBS). Endogenous peroxidases were quenched with 50 mmol/L NH_4Cl (30 minutes at room temperature), and antigen retrieval was performed by incubation of sections with hot 0.1 mol/L sodium citrate buffer (10 minutes at room temperature). Sections were blocked in 5% normal goat serum + 5% bovine serum albumin in PBS + 0.1% Triton X-100 and incubated with primary antibodies overnight at 4°C. Slides were washed 3 × 5 minutes in PBS and incubated with secondary antibodies in blocking buffer for 45 minutes at 37°C. Slides were washed 3 × 5 minutes in PBS, counterstained with DAPI, and coverslipped with 50% glycerol. All slides were imaged using a Zeiss LSM 800 confocal microscope with Airyscan superresolution (Dublin, CA). See Table 1 for dilutions of all primary and secondary antibodies.

DHE Staining

Reactive oxygen species were measured in retinal cryosections by dihydroethidium (DHE) staining. Enucleated eyes were dissected on ice-cold PBS, frozen in Tissue Tek OCT Compound within 15 minutes of enucleation, and cryosectioned at 10 μm. Slides were stored at −20°C and brought to room temperature before rehydration with 1 × PBS. Fresh frozen retinal cryosections spanning the optic nerve were incubated with DHE (Thermo Fisher, Waltham, MA; 1:5000) for 20 minutes, followed by counterstaining with DAPI (1:10,000).

Quantitative PCR

Gene expression of glucose transporters, inflammatory cytokines, and oxidative stress molecules was measured by quantitative PCR on dissected retinal tissue. RNA was extracted using the RNAeasy Mini Kit (Qiagen, Hilden, Germany; number 74104), and RT-PCR was performed using the Verso cDNA synthesis kit (Thermo Scientific; number AB1453A). Radiant Green 2X qPCR Lo-ROX enzyme (Alkali Scientific Inc., Fort Lauderdale, FL) was used for all real-time quantitative PCRs. Relative fold

Table 2 Primers

Gene	Forward primer	Reverse primer
Tnf	5′-CATCTTCTCAAAATTCGAGTGACAA-3′	5′-TGGGAGTAGACAAGGTACAACCC-3′
Il1b	5′-GATCCACACTCTCCAGCTGCA-3′	5′-CAACCAACAAGTGATATTCTCCATG-3′
Ptgs2 (Cox2)	5′-CACAGCCTACCAAAACAGCCA-3′	5′-GCTCAGTTGAACGCCTTTTGA-3′
Nos2	5′-GACTCTTGGTGAAAGTGGTGTTC-3′	5′-GCAGACAACCTTGGTGTTGA-3′
Actb	5′-TCATGAAGTGTGACGTTGACATCCGT-3′	5′-CCTAGAAGCATTTGCGGTGCACGATG-3′

changes in gene expression were determined using the comparative threshold cycle (C_T) method ($2\Delta\Delta C_T$ method). For all analyses, β-actin was used as the reference gene. Hypoxia-inducible factor (HIF)-1α (number QT01039542) and vascular endothelial growth factor (VEGF; number QT00160769) were analyzed using primers from Qiagen. Primers for all other genes investigated are listed in Table 2.

Statistical Analysis

For all experiments, data are presented as average ± SEM unless otherwise indicated. At least three mice per genotype/time point were utilized for all experiments. Statistical significance was determined by one- or two-way analysis of variance (ANOVA) with Tukey multiple comparisons test using GraphPad Prism 6 Software (Boston, MA). Western blot and real-time quantitative PCR analysis was performed using one-way ANOVA (genotype). Analysis of a-waves, b-waves, and the light-adapted response was performed using two-way ANOVA (genotype and flash intensity) for each time point. The c-wave and each OP was analyzed by one-way ANOVA (genotype) for each time point. No repeated-measures tests were performed.

Results

Glut1$^{+/+}$*Lepr*$^{db/db}$ mice on the C57BLKS background exhibit elevated body weight and blood glucose levels as early as 4 weeks of age.[8] When crossed with the *Glut1*$^{+/-}$ line to generate a *Glut1*$^{+/-}$*Lepr*$^{db/db}$ mouse, there was no change in the development of obesity (Figure 1A) or hyperglycemia (Figure 1B), despite the presence of only one Glut1 (*Slc2a1*) allele. *Glut1*$^{+/-}$ mice displayed a significant reduction in Glut1 levels, as depicted by Western blot analysis (Figure 1C) [$F(3,8) = 15.73$, $P = 0.0010$] and immunohistochemistry (Figure 1D). As previously shown, Glut1 was expressed throughout the retina, with high expression in the RPE and exclusion from the outer segments.[9] Notably, as observed in the streptozotocin-induced type 1 diabetic mouse retina,[7] Glut1 appeared to be elevated in the *Lepr*$^{db/db}$ retina.

Lepr$^{db/db}$ mice on the C57BLKS background initially display reductions to ERG b- and c-wave amplitudes at 8 weeks of age.[10] Herein, significant reductions were found in all ERG component amplitudes (including the a-wave) at 16 weeks. Therefore, to determine whether the reduction of Glut1 affected the onset and progression of ERG defects found in these mice, strobe flash electroretinography was conducted at both 8 and 16 weeks of age. A 10-step ERG protocol was performed on control (*Lepr*$^{db/+}$) and diabetic (*Lepr*$^{db/db}$) mice with wild type (*Glut1*$^{+/+}$) or reduced levels of Glut1 (*Glut1*$^{+/-}$). Figure 2A (8 weeks) and Figure 2C (16 weeks) depict representative waveform traces from step 9 of the protocol (1.4 log cd.s/m^2). As expected, no differences were observed between *Glut1*$^{+/+}$*Lepr*$^{db/+}$ and *Glut1*$^{+/-}$*Lepr*$^{db/+}$ mice, and *Glut1*$^{+/+}$*Lepr*$^{db/db}$ mice exhibited significant reductions in a- and b-wave amplitudes compared with controls (Figure 2, B and D) [ANOVAs by genotype: a-wave, $F(3, 229) = 12.53$, $P < 0.0001$; b-wave $F(3,229) = 14.02$, $P < 0.0001$). However, both components were fully normalized in *Glut1*$^{+/-}$*Lepr*$^{db/db}$ mice, at both ages (Figure 2, A–D). The average amplitude of each mouse cohort in response to all flash intensities is shown in the intensity response curves in Figure 2B (8 weeks) and Figure 2D (16 weeks). Importantly, no difference between *Glut1*$^{+/+}$*Lepr*$^{db/+}$ and *Glut1*$^{+/-}$*Lepr*$^{db/+}$ mice was observed in the scotopic light-evoked response to any flash luminance, at either age.

As reduced OP amplitudes and increased latency of these filtered wavelets are also characteristic of early DR, the OPs from each cohort of mice were analyzed at both ages. Figure 2, E and F, depicts the normalization of the OP amplitudes in the *Glut1*$^{+/-}$*Lepr*$^{db/db}$ mice compared with *Glut1*$^{+/+}$*Lepr*$^{db/db}$ mice (Figure 2, E and F) [ANOVAs by genotype: OP1 8 weeks, $F(3,15) = 6.673$, $P = 0.0044$; OP2 8 weeks, $F(3,16) = 5.656$, $P = 0.0077$; OP3 8 weeks, $F(3,16) = 8.653$, $P = 0.0012$; OP1 16 weeks, $F(3,11) = 7.846$, $P = 0.0045$; OP2 16 weeks, $F(3,11) = 24.58$, $P < 0.0001$; OP3 16 weeks, $F(3,11) = 11.40$, $P = 0.0011$]. Table 3 further demonstrates the significant increase in latency of OP2 and OP3 at 16 weeks in the *Glut1*$^{+/+}$*Lepr*$^{db/db}$ mice, which was normalized by the reduction of Glut1 in the *Glut1*$^{+/-}$*Lepr*$^{db/db}$ strain (Table 3) [ANOVA: OP2 16 weeks, $F(3,11) = 13.47$, $P = 0.0005$; OP3 16 weeks, $F(3,11) = 12.10$, $P = 0.0008$].

Dysfunction of the RPE is one of the earliest pathophysiological hallmarks of DR. To assess whether reduction of the Glut1 similarly prevents RPE dysfunction in T2D,

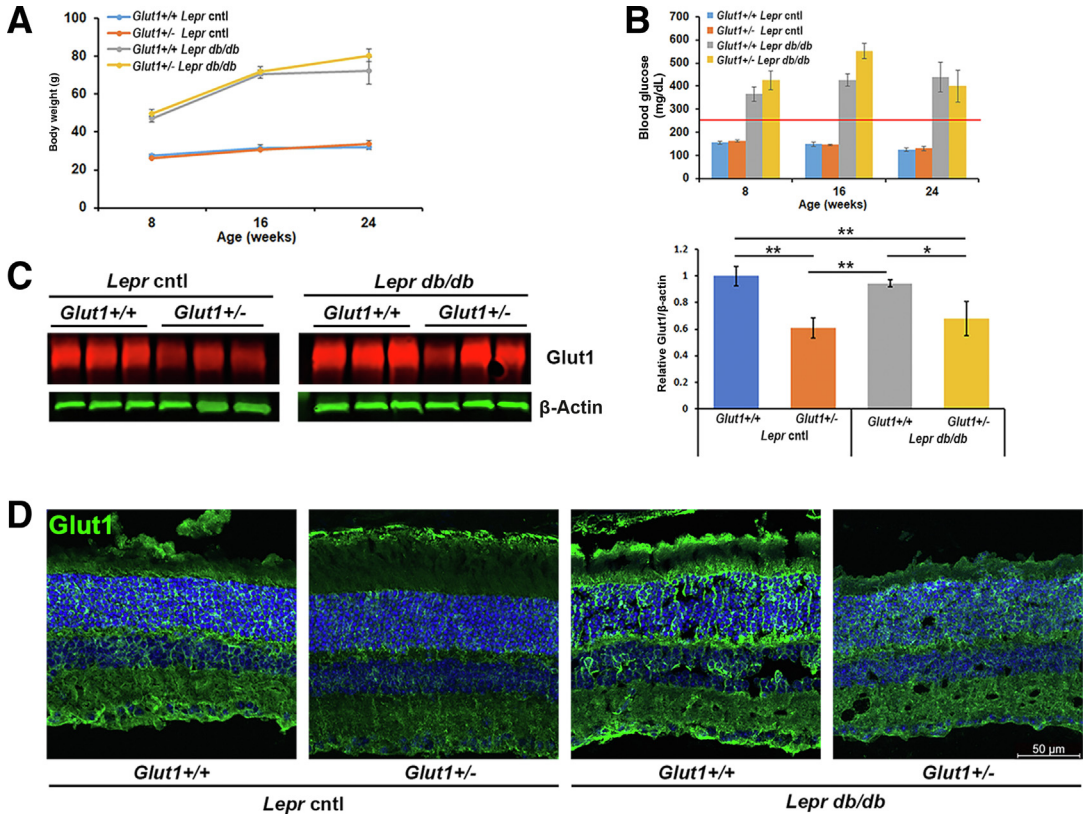

Figure 1 *Lepr*$^{db/db}$ mice exhibit obesity and hyperglycemia despite expression of one *Glut1* allele. **A:** Body weight of nondiabetic [*Lepr* control (cntl)] and diabetic (*Lepr*$^{db/db}$), Glut1 wild-type (*Glut1*$^{+/+}$) or heterozygous (*Glut1*$^{+/-}$) mice from 8 to 16 weeks of age. **B:** Nonfasting blood glucose. Measurements >250 mg/dL were considered hyperglycemic. **Red line** indicates threshold for hyperglycemia (250 mg/dL). **C:** Protein levels of Glut1 from dissected retinas of 16-week—old mice. Retinas were dissected, and total Glut1 levels were normalized to β-actin for quantitative analysis. **D:** Confocal images of Glut1 immunoreactivity (green) and DAPI counterstaining (blue) in cryosections from retinas at 16 weeks of age. $n \geq 3$ in each group (**C**). $^{*}P \leq 0.05$, $^{**}P \leq 0.01$. Scale bar = 50 μm (**D**).

c-wave amplitudes evoked in response to a 5-cd.s/m^2 light stimulus (Figure 3) were analyzed. Representative waveforms are depicted in Figure 3, A and C. As observed in response to the strobe flash stimulus, i) no differences in response were identified in c-wave amplitudes between *Glut1*$^{+/+}$*Lepr*$^{db/+}$ and *Glut1*$^{+/-}$*Lepr*$^{db/+}$ mice, ii) *Glut1*$^{+/+}$*Lepr*$^{db/db}$ mice exhibited a significant reduction in c-wave amplitude compared with both nondiabetic controls, and iii) c-wave amplitudes of *Glut1*$^{+/-}$*Lepr*$^{db/db}$ mice were fully normalized (Figure 3, B and D) [ANOVA by genotype: F(3, 208) = 13.98, $P < 0.0001$].

Cone photoreceptor function can be evaluated by the photopic light-adapted response. Following the c-wave, mice were light adapted for 7 minutes before another strobe flash stimulus (Figure 4). At 8 weeks of age, the light-adapted responses of the *Glut1*$^{+/+}$*Lepr*$^{db/db}$ mice were reduced (Figure 4A), but not to the same extent as the dark-adapted responses, or the c-wave. However, at both 8 and 16 weeks of age (Figure 4C; when a significant reduction in the light-adapted response of *Glut1*$^{+/+}$*Lepr*$^{db/db}$ mice was identified), *Glut1*$^{+/-}$*Lepr*$^{db/db}$ responses were restored (Figure 4, B and D) [ANOVA by genotype: F(3, 227) = 4.570, $P = 0.004$].

To determine whether systemic reduction of Glut1 also affected presence of oxidative stress and inflammation in the retina of *Lepr*$^{db/db}$ mice, expression of oxidative stress molecules cyclooxygenase-2 (Cox2) and nitric oxide synthase 2 (Nos2) (Figure 5, A and B) was analyzed. Expression of each gene was significantly elevated in *Glut1*$^{+/+}$*Lepr*$^{db/db}$ retinas compared with nondiabetic controls, and levels were normalized in retinas dissected from *Glut1*$^{+/-}$*Lepr*$^{db/db}$ mice [Cox2, F(3, 8) = 8.723, $P = 0.0067$;Nos2, F(3, 8) = 17.59, $P = 0.0007$] (Figure 5, A and B). To further evaluate the presence of superoxide production in the retina, fresh frozen sections incubated with DHE were evaluated. Figure 5C depicts elevated levels of DHE throughout the inner nuclear layer, outer nuclear layer, and outer segments of *Glut1*$^{+/+}$*Lepr*$^{db/db}$ retinas compared with nondiabetic controls and *Glut1*$^{+/-}$*Lepr*$^{db/db}$ mice.

The expression of classic inflammatory cytokines, IL-1β and tumor necrosis factor (TNF)-α (Figure 6, A and B), and pro-angiogenic factors, HIF-1α and VEGF (Figure 6, C and D) was analyzed next. Expression of each gene was significantly increased in *Glut1*$^{+/+}$*Lepr*$^{db/db}$ retinas compared with nondiabetic controls, and levels were normalized in retinas dissected from *Glut1*$^{+/-}$*Lepr*$^{db/db}$ mice

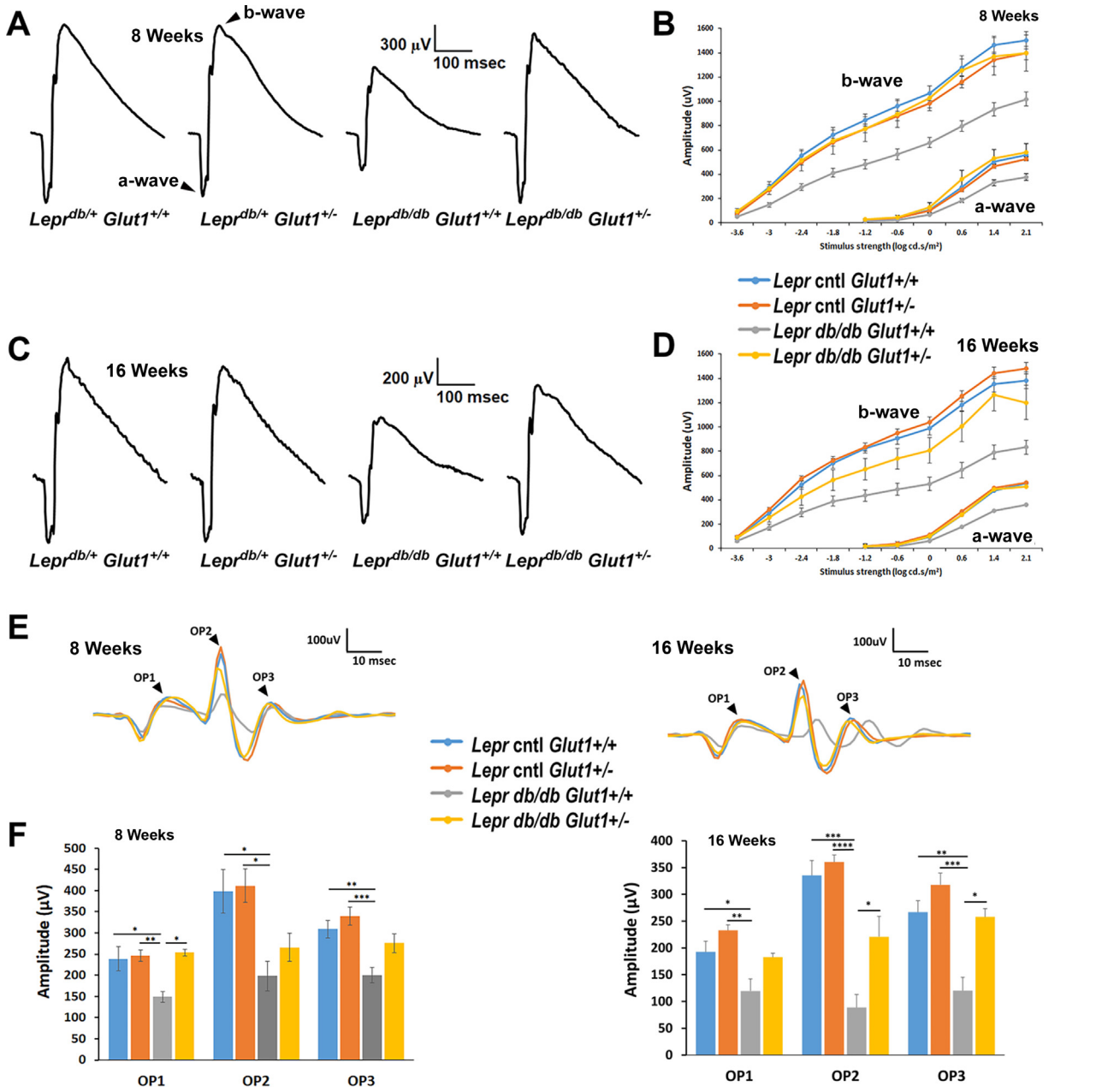

Figure 2 Diabetes-induced electroretinogram (ERG) defects are normalized in mice with reduced Glut1. **A**–**F:** Strobe flash ERGs were performed on nondiabetic [*Lepr* control (cntl)] and diabetic (*Lepr*$^{db/db}$), Glut1 wild-type (*Glut1*$^{+/+}$) or heterozygous (*Glut1*$^{+/-}$) mice at both 8 and 16 weeks of age. **A** and **C:** Representative strobe flash ERG waveform traces evoked in response to a 1.4 log cd.s/m^2 light stimulus are depicted from testing at 8 (**A**) and 16 (**C**) weeks. **B** and **D:** Luminance-response functions for the a- and b-wave. **E:** Representative traces of filtered oscillatory potentials (OPs) from strobe flash ERGs evoked by a 1.4 log cd.s/m^2 flash stimulus at 8 (**left side**) and 16 (**right side**) weeks of age. **F:** Average amplitude of OP1, OP2, and OP3 at 8 (**left side**) and 16 (**right side**) weeks of age. Amplitude was measured from the minimum of the preceding trough to the peak of the potential. *$P \leq 0.05$, **$P \leq 0.01$, ***$P \leq 0.001$, and ****$P \leq 0.0001$.

[IL-1β, $F(3, 10) = 56.23$, $P < 0.0001$;TNF-α, $F(3, 8) = 11.24$, $P = 0.0031$;HIF-1α, $F(3, 8) = 33.60$, $P < 0.0001$;VEGF, $F(3, 9) = 11.60$, $P = 0.0019$] (Figure 6, A–D). To assess the activation status of Müller glia in the *Glut1*$^{+/+}$*Lepr*$^{db/db}$ retina, immunohistochemistry was performed on retinal cryosections using an anti–glutamine synthetase antibody (Figure 6E). As expected, in the *Glut1*$^{+/+}$*Lepr*$^{db/db}$ retina, staining was observed from the external limiting membrane to the ganglion cell layer, spanning the length of the Müller glia. However, immunoreactivity was primarily limited to Müller glia end feet (and autofluorescent blood vessels) in all other cohorts. These data demonstrate that reduction of Glut1 prevents both functional defects of the diabetic retina as well as the development of inflammation and oxidative stress.

Table 3 Diabetes Does Not Alter OP Latency with or without Reduction in Glut1

Age, weeks	Genotype	Oscillatory potential latency, average ± SEM, milliseconds (*n*)		
		OP1	OP2	OP3
8	*Glut1*$^{+/+}$ *Lepr* cntl	11.37 ± 0.277 (6)	23.30 ± 0.372 (6)	34.25 ± 0.397 (6)
8	*Glut1*$^{+/+}$ *Lepr db/db*	11.81 ± 0.485 (5)	23.80 ± 0.424 (5)	34.61 ± 0.564 (5)
8	*Glut1*$^{+/-}$ *Lepr* cntl	11.09 ± 0.277 (6)	23.57 ± 0.411 (6)	33.83 ± 0.668 (6)
8	*Glut1*$^{+/-}$ *Lepr db/db*	11.09 ± 0.734 (3)	23.02 ± 0.999 (3)	34.39 ± 1.544 (3)
16	*Glut1*$^{+/+}$ *Lepr* cntl	12.06 ± 0.277 (4)	24.13 ± 0.555 (4)	35.36 ± 0.734 (4)
16	*Glut1*$^{+/+}$ *Lepr db/db*	11.23 ± 0.537 (4)	27.04 ± 0.240 (4)*,†	38.27 ± 0.588 (4)†,‡
16	*Glut1*$^{+/-}$ *Lepr* cntl	10.82 ± 0.215 (4)	23.30 ± 0.588 (4)	33.70 ± 0.712 (4)
16	*Glut1*$^{+/-}$ *Lepr db/db*	11.09 ± 0.277 (3)	23.30 ± 0.480 (3)‡	33.02 ± 0.548 (3)§

Cntl, control; OP, oscillatory potential.
*$P < 0.01$, Glut1$^{+/+}$ *Lepr* cntl versus Glut1$^{+/+}$ *Lepr* db/db.
†$P < 0.01$, Glut1$^{+/-}$ *Lepr* cntl versus Glut1$^{+/+}$ *Lepr* db/db.
‡$P < 0.05$, Glut1$^{+/+}$ *Lepr* cntl versus Glut1$^{+/+}$ *Lepr* db/db.
§$P < 0.01$, Glut1$^{+/+}$ *Lepr* db/db versus Glut1$^{+/-}$ *Lepr* db/db.

Discussion

This study demonstrates, for the first time, that moderate, systemic reduction of Glut1 is effective in preventing retinal pathophysiology in a mouse model of T2D. All previous work to date investigating the therapeutic potential for Glut1 in DR utilized mouse models of type 1 diabetes.[7,11–13] Therefore, the findings presented here are critically important as, of the one-third of diabetic patients who will develop DR, 90% to 95% experience T2D.[14,15]

Functional retinal defects, neurodegeneration, and inflammation were first identified in the *Lepr*$^{db/db}$ spontaneous T2D mouse model by Bogdanov et al[16] in 2014, establishing early neuronal involvement as a hallmark of DR in T2D. This study also demonstrated that caloric restriction, which reduced hyperglycemia in the mice, led to a normalization of ERG OP latency and amplitude, reduced retinal inflammation, and prevented ganglion cell death.[16] Recently, *in vivo* ERGs from 3- and 6-month–old *Lepr*$^{db/db}$ mice demonstrated reductions in a- and b-wave amplitudes only at 6 months.[17] When compared with *ex vivo* ERGs performed on retinas dissected at the same age, normal light-evoked responses were recorded from retinas cultured in a normoglycemic environment. These findings revealed that extrinsic factors induced the functional defects in *Lepr*$^{db/db}$ diabetic mice, indicating that the defects are reversible.

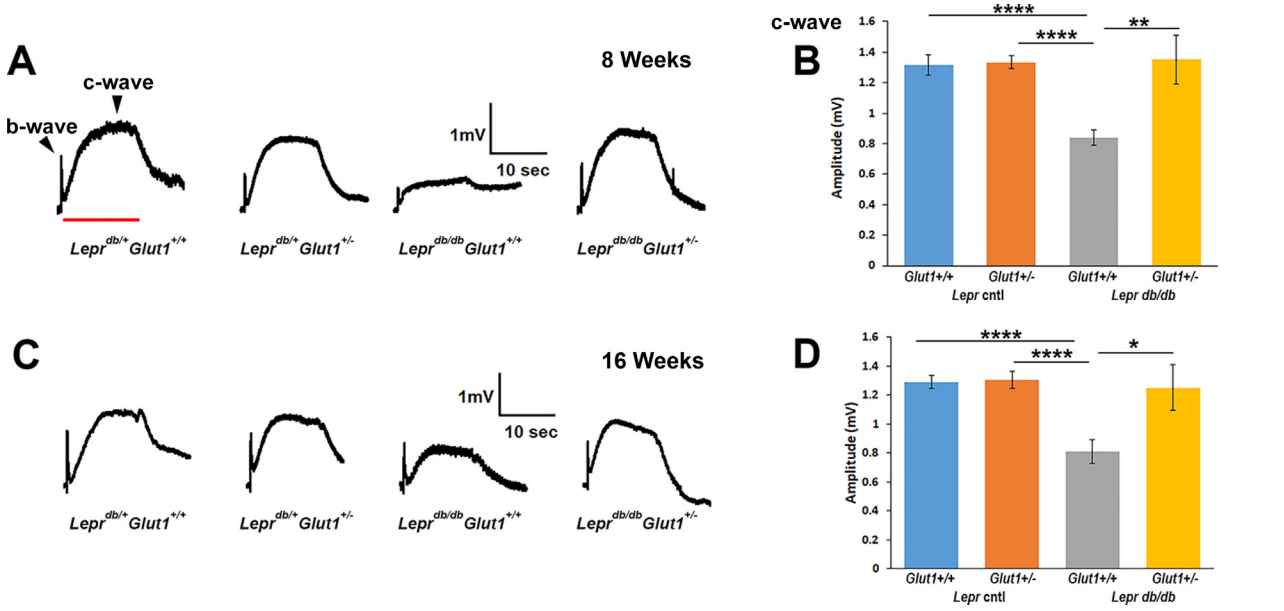

Figure 3 Retinal pigment epithelium defects are ameliorated in diabetic *Glut1*$^{+/-}$ mice. **A** and **C:** Representative waveforms induced by a 5-cd/m^2 white stimulus for 10 seconds. **Red line** indicates duration of light stimulus. **B** and **D:** Average amplitude of the c-wave at 8 and 16 weeks of age. Amplitude of the c-wave was determined by subtracting the average baseline amplitude from the maximal response following the b-wave. *$P \leq 0.05$, **$P \leq 0.01$, and ****$P \leq 0.0001$. Cntl, control.

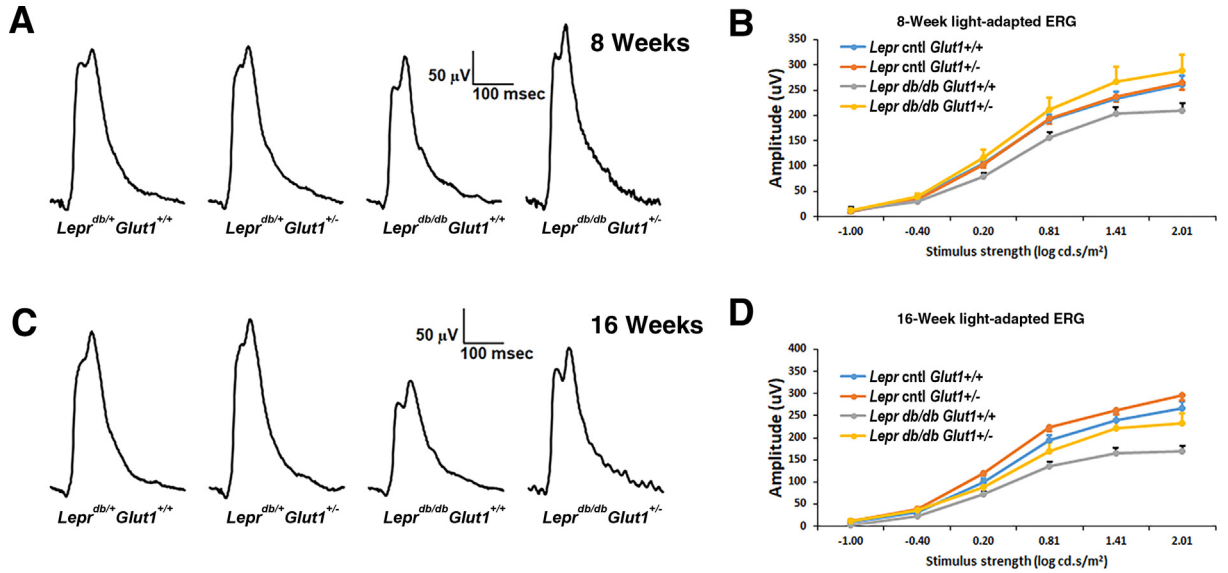

Figure 4 Photopic electroretinogram (ERG) defects are normalized in diabetic *Glut1*$^{+/-}$ mice. **A** and **C:** Representative light-adapted ERG waveform traces evoked by a 1.4 log cd.s/m^2 light stimulus superimposed over the adapting field. **B** and **D:** Luminance-response function for the light-adapted responses at 8 (**B**) and 16 (**D**) weeks of age. Amplitudes were calculated by summing the peak of the waveform with the amplitude at 8.3 milliseconds. Cntl, control.

Indeed, the current findings demonstrated that reducing Glut1 normalized ERG defects seen at 8 and 16 weeks in *Lepr*$^{db/db}$ mice. However, the mice remained severely obese despite the reduction in Glut1 and were difficult to maintain through 24 weeks. Of the mice that did survive, electroretinograms were similarly restored to normal amplitudes (data not shown). These findings suggest that obesity (and presumably hyperlipidemia) does not overtly contribute to retinal dysfunction associated with DR and that glucose transport into the retina or retinal glucose metabolism can be utilized as a primary target for intervention.

It has been suggested that oxidative stress both contributes to and is a consequence of metabolic dysfunction associated with DR.[18] Evidence of oxidative stress in *Lepr*$^{db/db}$ mice has been observed as early as 8 weeks of age,[16] and glial activation was increased in diabetic mice at all ages/time points examined. Herein, elevated levels of inflammatory cytokines, oxidative stress molecules, and pro-angiogenic factors were found at 16 weeks of age. Moreover, glutamine synthetase elevation in Müller glia demonstrated a neuroprotective effect by these cells. Bogdanov et al[16] found elevated levels of *Slc38a1*, the glutamine transporter. These increases in both glutamine synthetase and the glutamine transporter demonstrate that the diabetic retina is attempting to combat elevations in glutamate to prevent neural toxicity and cell death. More importantly, in addition to the prevention of ERG defects, *Glut1*$^{+/-}$*Lepr*$^{db/db}$ mice displayed low levels of glutamine synthetase, superoxide production (DHE), as well as control expression levels of *IL-1β*, *TNF-α*, *VEGF*, *HIF-1α*, *Cox2*, and *Nos2* (Figure 5), indicating that both functional defects as well as molecular signatures of diabetic retinas (reactive oxygen species and inflammation) are normalized by reducing Glut1.

An increase in Glut1 has been demonstrated in the streptozotocin-induced diabetic retina.[7] Here, the study shows a similar trend for increased Glut1 throughout the *Glut1*$^{+/+}$*Lepr*$^{db/db}$ retina (Figure 1, C and D), which was not observed in the *Glut1*$^{+/-}$*Lepr*$^{db/db}$ mice. These findings indicate that a glucose-induced increase in Glut1 may drive the elevation. When glucose transport to the retina is limited by the systemic reduction in Glut1 caused by loss of one *Slc2a1* allele, Glut1 is not increased. This follows the premise of glucose-induced glucose uptake more commonly observed occurring via Glut4 in muscle, fat, and heart, where glucose is insulin-regulated.[19] Future investigations will determine whether Glut1 levels are altered by insulin signaling in the retina and whether Glut1 activity, rather than expression, can also be modulated to prevent DR.

Notably, the use of a mouse strain that expresses only one Glut1 allele to induce reduction of Glut1 provides a means to extrapolate our findings to hypothesize how a moderate, systemic inhibition of Glut1 achieved via pharmacology could be utilized for prevention of DR. Cancer therapies already utilize Glut1-specific and pan-Glut inhibitors to combat the increased proliferation of neoplastic cells.[20,21] Cancer cells utilize the same metabolic paradigm as the retina, relying primarily on glycolysis (also known as the Warburg effect), and a promising new field of chemotherapy for cancer is the inhibition of Glut-mediated transport of glucose to starve tumors.

Interestingly, many therapeutics identified to reduce or prevent characteristics of DR are known Glut inhibitors also used in anti-neoplastic cancer studies.[20] Among these include curcumin,[22,23] genistein,[24–26] quercetin,[27–29] and resveratrol.[30–33] Some inhibit Glut1 at the gene/protein level (genistein and resveratrol), whereas others also

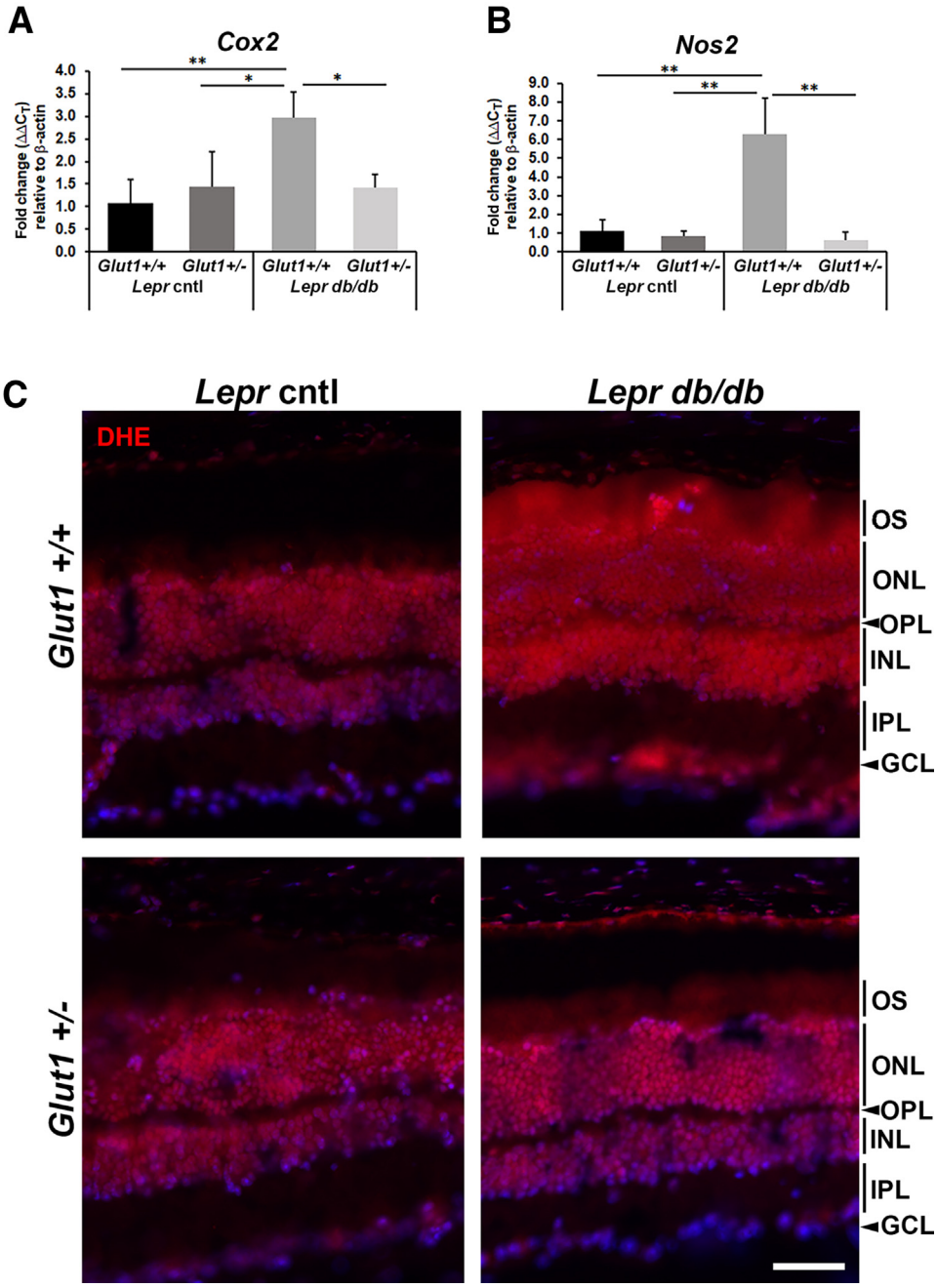

Figure 5 Oxidative stress is reduced in diabetic *Glut1*$^{+/-}$ mice. **A** and **B:** Quantification of oxidative stress mediators [*Cox2* (**A**) and *Nos2* (**B**)] at 16 weeks of age. Relative fold changes in gene expression were determined using the $2\Delta\Delta C_T$ method. Both genes were normalized to expression of β-*actin* and compared with expression in *Lepr*$^{db/+}$*Glut1*$^{+/+}$ mice. **C:** Confocal microscopy of fresh frozen retinal cryosections from 24-week—old mice stained with dihydroethidium (DHE; red). *$P \leq 0.05$, **$P \leq 0.01$. Scale bar = 50 μm (**C**). Cntl, control; GCL, ganglion cell layer; INL, inner nuclear layer; IPL, inner plexiform layer; ONL, outer nuclear layer; OPL, outer plexiform layer; OS, outer segments.

noncompetitively (resveratrol) or competitively inhibit Glut1 (quercetin).[20] Many of these compounds are also polyphenols and may exert their actions through multiple mechanisms, including targeting of cell signaling, hormonal regulation, and anti-oxidation. The lipid/cholesterol drug, fenofibrate, which has also emerged as a promising treatment for DR among patients with T2D,[34] similarly reduces Glut1 levels in cancer cells.[35] Much like the current findings of normalized retinal pathophysiology by reducing Glut1, it has been shown to be effective for DR despite sustained hyperlipidemia.

Whether by use of a naturally occurring compound, or synthetically generated small-molecule inhibitor, *moderated* targeting of glucose transport is essential as the reduction of

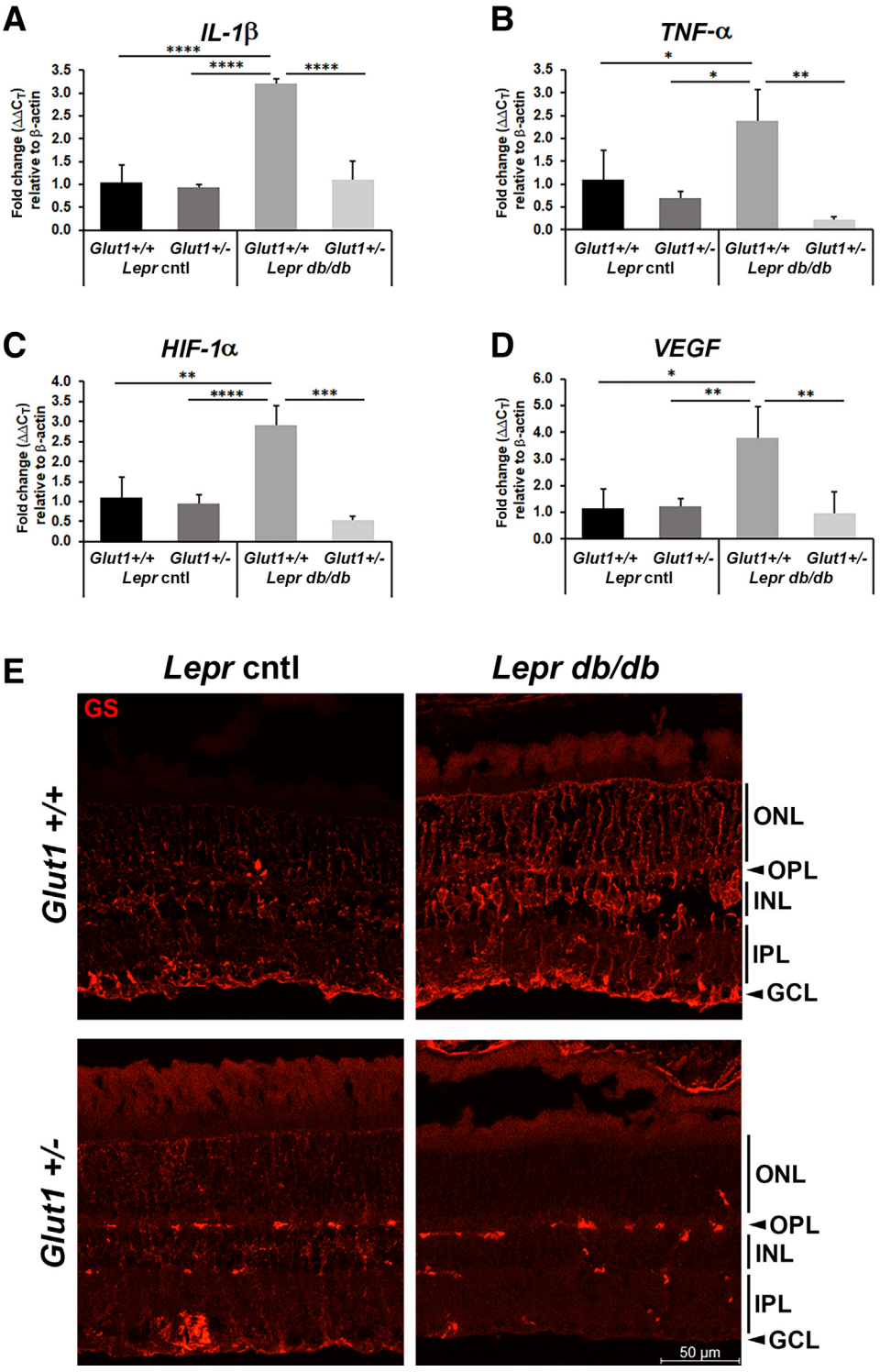

Figure 6 Inflammatory cytokines are not elevated in diabetic *Glut1*$^{+/-}$ mice. **A**—**D:** Quantification of inflammatory cytokines [*IL-1β* (**A**) and *TNF-α* (**B**)] and pro-angiogenic factors [*HIF-1α* (**C**) and *VEGF* (**D**)] at 16 weeks of age. Relative fold changes in gene expression were determined using the $2\Delta\Delta C_T$ method. All genes were normalized to expression of β-*actin* and compared with expression in *Lepr*$^{db/+}$*Glut1*$^{+/+}$ mice. **E:** Confocal microscopy of retinal cryosections from 16-week—old mice stained with anti—glutamine synthetase (red). $^{*}P \leq 0.05$, $^{**}P \leq 0.01$, $^{***}P \leq 0.001$, and $^{****}P \leq 0.0001$. Scale bar = 50 μm (**E**). Cntl, control; GCL, ganglion cell layer; INL, inner nuclear layer, IPL, inner plexiform layer; ONL, outer nuclear layer; OPL, outer plexiform layer.

glucose levels in the brain beyond normoglycemia is detrimental. Systemically, loss of a single Glut1 allele in humans leads to Glut1 deficiency syndrome, characterized by seizures, reduced locomotion, abnormal brain microvasculature, micrencephaly, neuroinflammation, developmental delay, and speech/language impairments. This sequelae of symptoms arises from insufficient glucose in the brain for neuronal metabolism.[36,37] However, in a mouse model of Glut1

deficiency syndrome, when Glut1 reduction is induced in adult mice rather than at birth, the pathologic phenotypes of Glut1 deficiency syndrome are prevented.[38] Therefore, as reduction of Glut1 in diabetic patients would be initiated after development is complete, targeting of Glut1 is a viable treatment option.

With specific regard to retinal function, although sustained hypoglycemia within the retina leads to age-related vision loss, characterized by reduced visual acuity, ERG amplitudes, and death of inner retinal neurons,[39] acute hypoglycemia in individuals with or without diabetes induced reversible reductions in ERG amplitudes, appearance of scotomas, and reduced contrast sensitivity. All perturbations in vision and retinal function were stabilized on euglycemia.[40] The use of precision pharmacology and nanoconcentrations of Glut1 inhibitors for the treatment of DR can ensure glucose concentrations are titrated to normal endogenous levels. Alternatively, topical ocular treatment with Glut1 inhibitors may be considered. Future studies will utilize data from anti-cancer drug trials to design a treatment paradigm using Glut1 inhibitors for the determination of whether systemic, pharmacologic inhibition of Glut1 can also be harnessed to prevent or treat DR. Looking toward whole-body treatment of Glut1 inhibition for T2D, which may also be relevant for the other microvascular complications of diabetes (neuropathy and nephropathy) as well as the macrovascular complications associated with diabetes (eg, coronary heart disease and cerebrovascular disease), it will be important in translation to clinical research to i) begin Glut1 inhibition early, ii) concomitantly treat the mice for comorbidities, such as obesity, and iii) determine how a multipharmacologic approach to treating T2D affects *Slc2a1* expression, Glut1 levels, and Glut1 activity in the retina (and other tissues).

In sum, the current findings demonstrate that a moderate, systemic reduction of Glut1 inhibits both functional retinal defects observed by electroretinography and the molecular signatures of retinal oxidative stress and inflammation characteristic of the $Lepr^{db/db}$ mouse model of type 2 diabetes. These data are significant as 95% of patients with diabetes experience type 2 diabetes, and preclinical investigations for therapies must address this group.

Acknowledgments

We thank Dr. Neal Peachey, Dr. Lin Mei, and Dr. Wen-Cheng Xiong for supporting these experiments.

References

1. Eid SA, O'Brien PD, Hinder LM, Hayes JM, Mendelson FE, Zhang H, Zeng L, Kretzler K, Narayanan S, Abcouwer SF, Brosius III FC 3rd, Pennathur S, Savelieff MG, Feldman EL: Differential effects of empagliflozin on microvascular complications in murine models of type 1 and type 2 diabetes. Biology 2020, 9:347
2. El Mouhayyar C, Riachy R, Khalil AB, Eid A, Azar S: SGLT2 inhibitors, GLP-1 agonists, and DPP-4 inhibitors in diabetes and microvascular complications: a review. Int J Endocrinol 2020, 2020:1762164
3. Gong Q, Zhang R, Wei F, Fang J, Zhang J, Sun J, Sun Q, Wang H: SGLT2 inhibitor-empagliflozin treatment ameliorates diabetic retinopathy manifestations and exerts protective effects associated with augmenting branched chain amino acids catabolism and transportation in db/db mice. Biomed Pharmacother 2022, 152:113222
4. Mima A: Renal protection by sodium-glucose cotransporter 2 inhibitors and its underlying mechanisms in diabetic kidney disease. J Diabetes Complications 2018, 32:720−725
5. Sha W, Wen S, Chen L, Xu B, Lei T, Zhou L: The role of SGLT2 inhibitor on the treatment of diabetic retinopathy. J Diabetes Res 2020, 2020:8867875
6. Chen H, Zhang X, Liao N, Ji Y, Mi L, Gan Y, Su Y, Wen F: Decreased expression of glucagon-like peptide-1 receptor and sodium-glucose co-transporter 2 in patients with proliferative diabetic retinopathy. Front Endocrinol 2022, 13:1020252
7. Holoman NC, Aiello JJ, Trobenter TD, Tarchick MJ, Kozlowski MR, Makowski ER, De Vivo DC, Singh C, Sears JE, Samuels IS: Reduction of Glut1 in the neural retina but not the RPE alleviates polyol accumulation and normalizes early characteristics of diabetic retinopathy. J Neurosci 2021, 41:3275−3299
8. Hummel KP, Dickie MM, Coleman DL: Diabetes, a new mutation in the mouse. Science 1966, 153:1127−1128
9. Gospe SM 3rd, Baker SA, Arshavsky VY: Facilitative glucose transporter Glut1 is actively excluded from rod outer segments. J Cell Sci 2010, 123:3639−3644
10. Samuels IS, Bell BA, Pereira A, Saxon J, Peachey NS: Early retinal pigment epithelium dysfunction is concomitant with hyperglycemia in mouse models of type 1 and type 2 diabetes. J Neurophysiol 2015, 113:1085−1099
11. Lu L, Seidel CP, Iwase T, Stevens RK, Gong YY, Wang X, Hackett SF, Campochiaro PA: Suppression of GLUT1; a new strategy to prevent diabetic complications. J Cell Physiol 2013, 228:251−257
12. You ZP, Xiong B, Zhang YL, Shi L, Shi K: Forskolin attenuates retinal inflammation in diabetic mice. Mol Med Rep 2018, 17:2321−2326
13. You ZP, Zhang YL, Shi K, Shi L, Zhang YZ, Zhou Y, Wang CY: Suppression of diabetic retinopathy with GLUT1 siRNA. Sci Rep 2017, 7:7437
14. Lee R, Wong TY, Sabanayagam C: Epidemiology of diabetic retinopathy, diabetic macular edema and related vision loss. Eye Vis 2015, 2:17
15. Zheng Y, He M, Congdon N: The worldwide epidemic of diabetic retinopathy. Indian J Ophthalmol 2012, 60:428−431
16. Bogdanov P, Corraliza L, Villena JA, Carvalho AR, Garcia-Arumi J, Ramos D, Ruberte J, Simo R, Hernandez C: The db/db mouse: a useful model for the study of diabetic retinal neurodegeneration. PLoS One 2014, 9:e97302
17. Becker S, Carroll LS, Vinberg F: Rod phototransduction and light signal transmission during type 2 diabetes. BMJ Open Diabetes Res Care 2020, 8:e001571
18. Kang Q, Yang C: Oxidative stress and diabetic retinopathy: molecular mechanisms, pathogenetic role and therapeutic implications. Redox Biol 2020, 37:101799
19. Chang L, Chiang SH, Saltiel AR: Insulin signaling and the regulation of glucose transport. Mol Med 2004, 10:65−71
20. Temre MK, Kumar A, Singh SM: An appraisal of the current status of inhibition of glucose transporters as an emerging antineoplastic approach: promising potential of new pan-GLUT inhibitors. Front Pharmacol 2022, 13:1035510
21. Zambrano A, Molt M, Uribe E, Salas M: Glut 1 in cancer cells and the inhibitory action of resveratrol as a potential therapeutic strategy. Int J Mol Sci 2019, 20:3374
22. Aldebasi YH, Aly SM, Rahmani AH: Therapeutic implications of curcumin in the prevention of diabetic retinopathy via modulation of anti-oxidant activity and genetic pathways. Int J Physiol Pathophysiol Pharmacol 2013, 5:194−202

23. Yang J, Miao X, Yang FJ, Cao JF, Liu X, Fu JL, Su GF: Therapeutic potential of curcumin in diabetic retinopathy (review). Int J Mol Med 2021, 47:75
24. Elgayar SA, Eltony SA, Sayed AA, Abdel-Rouf MM: Genistein treatment confers protection against gliopathy and vasculopathy of the diabetic retina in rats. Ultrastruct Pathol 2015, 39:385−394
25. Ibrahim AS, El-Shishtawy MM, Pena A Jr, Liou GI: Genistein attenuates retinal inflammation associated with diabetes by targeting of microglial activation. Mol Vis 2010, 16:2033−2042
26. Yousefi H, Komaki A, Shahidi S, Habibi P, Sadeghian R, Ahmadiasl N, Daghigh F: Diabetic neovascularization defects in the retina are improved by genistein supplementation in the ovariectomized rat. Inflammopharmacology 2021, 29:1579−1586
27. Chai GR, Liu S, Yang HW, Chen XL: Quercetin protects against diabetic retinopathy in rats by inducing heme oxygenase-1 expression. Neural Regen Res 2021, 16:1344−1350
28. Kumar B, Gupta SK, Nag TC, Srivastava S, Saxena R, Jha KA, Srinivasan BP: Retinal neuroprotective effects of quercetin in streptozotocin-induced diabetic rats. Exp Eye Res 2014, 125:193−202
29. Wang S, Du S, Wang W, Zhang F: Therapeutic investigation of quercetin nanomedicine in a zebrafish model of diabetic retinopathy. Biomed Pharmacother 2020, 130:110573
30. Ahmad I, Hoda M: Attenuation of diabetic retinopathy and neuropathy by resveratrol: review on its molecular mechanisms of action. Life Sci 2020, 245:117350
31. Chen Y, Meng J, Li H, Wei H, Bi F, Liu S, Tang K, Guo H, Liu W: Resveratrol exhibits an effect on attenuating retina inflammatory condition and damage of diabetic retinopathy via PON1. Exp Eye Res 2019, 181:356−366
32. Soufi FG, Mohammad-Nejad D, Ahmadieh H: Resveratrol improves diabetic retinopathy possibly through oxidative stress - nuclear factor kappaB - apoptosis pathway. Pharmacol Rep 2012, 64:1505−1514
33. Toro MD, Nowomiejska K, Avitabile T, Rejdak R, Tripodi S, Porta A, Reibaldi M, Figus M, Posarelli C, Fiedorowicz M: Effect of resveratrol on in vitro and in vivo models of diabetic retinophathy: a systematic review. Int J Mol Sci 2019, 20:3503
34. Keech AC, Mitchell P, Summanen PA, O'Day J, Davis TM, Moffitt MS, Taskinen MR, Simes RJ, Tse D, Williamson E, Merrifield A, Laatikainen LT, d'Emden MC, Crimet DC, O'Connell RL, Colman PG; FIELD Study Investigators: Effect of fenofibrate on the need for laser treatment for diabetic retinopathy (FIELD study): a randomised controlled trial. Lancet 2007, 370:1687−1697
35. Chen L, Peng J, Wang Y, Jiang H, Wang W, Dai J, Tang M, Wei Y, Kuang H, Xu G, Xu H, Zhou F: Fenofibrate-induced mitochondrial dysfunction and metabolic reprogramming reversal: the anti-tumor effects in gastric carcinoma cells mediated by the PPAR pathway. Am J Transl Res 2020, 12:428−446
36. Klepper J, Akman C, Armeno M, Auvin S, Cervenka M, Cross HJ, De Giorgis V, Della Marina A, Engelstad K, Heussinger N, Kossoff EH, Leen WG, Leiendecker B, Monani UR, Oguni H, Neal E, Pascual JM, Pearson TS, Pons R, Scheffer IE, Veggiotti P, Willemsen M, Zuberi SM, De Vivo DC: Glut1 deficiency syndrome (Glut1DS): state of the art in 2020 and recommendations of the international Glut1DS study group. Epilepsia Open 2020, 5:354−365
37. Tang M, Monani UR: Glut1 deficiency syndrome: new and emerging insights into a prototypical brain energy failure disorder. Neurosci Insights 2021, 16:26331055211011507
38. Tang M, Park SH, Petri S, Yu H, Rueda CB, Abel ED, Kim CY, Hillman EM, Li F, Lee Y, Ding L, Jagadish S, Frankel WN, De Vivo DC, Monani UR: An early endothelial cell-specific requirement for Glut1 is revealed in Glut1 deficiency syndrome model mice. JCI Insight 2021, 6:e145789
39. Umino Y, Everhart D, Solessio E, Cusato K, Pan JC, Nguyen TH, Brown ET, Hafler R, Frio BA, Knox BE, Engbretson GA, Haeri M, Cui L, Glenn AS, Charron MJ, Barlow RB: Hypoglycemia leads to age-related loss of vision. Proc Natl Acad Sci U S A 2006, 103:19541−19545
40. Khan MI, Barlow RB, Weinstock RS: Acute hypoglycemia decreases central retinal function in the human eye. Vis Res 2011, 51:1623−1626